

Chapter 4

Large-Scale Cyclic Polybutadiene Synthesis

4.0 – Abstract

The importance of polybutadiene (PBd) as a commercial material and a model system in fundamental research is discussed. A process for producing cyclic PBd via REMP and on scale was desired. Small-scale optimization experiments for the REMP of COD to PBd using a supported molecular REMP catalyst were pursued. A large-scale REMP reactor and recycling process were devised. The REMP recycling process succeeded twice in producing multi gram quantities of PBd, which vastly exceeded previous capabilities. The purity of cyclic PBd was established using IC. Unusual *cis*-selectivity in COD REMP reactions was observed.

Chapter 4 Acknowledgments

Bob Grubbs, Alice Chang, Dick Pederson and Adam Johns (Materia, Inc.)

Anthony Ndiripo and Prof. Harald Pasch (U. of Stellenbosch, S. Africa)

4.1 – Introduction

Polybutadiene

Polybutadiene (PBd) represents a substantial portion of all polymers produced worldwide, with over 3 trillion kg produced in 2015 alone. Approximately 70% of PBd produced globally goes into the manufacture of automobile tires, with the remaining share composing a wide variety of plastics and rubbers. PBd synthetic strategies provide microstructure control to achieve the desired 1,4-*cis*-insertion, 1,4-*trans*-insertion, and 1,2-insertion composition for modulating material properties. High-*cis* PBd generally comes from organolithium-mediated anionic polymerization, while high-*trans* generally comes from Ziegler-Natta α -olefin polymerization catalysts (Fig 4.1). Commercial PBd always contains some of the branched 1,2-insertion component, which is used to enhance toughness of PBd through cross-linking. Copolymerization of butadiene with styrene provides styrene-butadiene rubber (SBR), which is the most common material in automobile tires.¹

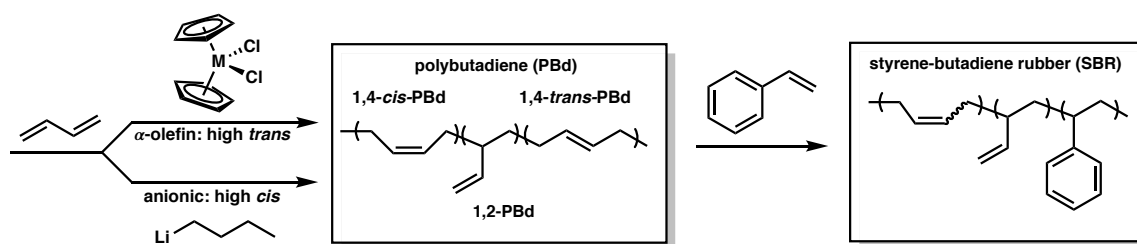


Figure 4.1 | Industrial production of PBd and SBR via either metallocene catalysts (M = Zr, Ti, Hf) or organolithium species to furnish high *trans* or high *cis* PBd, respectively.

Cyclic PBd and PS have been used as model systems for studying cyclic polymer melt-state viscoelastic properties, namely their rheological behavior.²⁻⁶ The cycles used in these studies required a ring-closure strategy, followed by topological purification with preparative interaction chromatography (IC). Trace linear impurity has long been known to drastically alter cyclic polymer rheological responses, with 0.07% linear PS detectable by stress relaxation measurements.⁷

The first, and still only, report of cyclic polybutadiene from olefin metathesis came from our group in 2003.⁸ Numerous reports of linear PBd from ROMP, including telechelic PBd^{9,10} and PBd copolymers,^{11,12} emerged from our group, and others, beginning in the 1990's (Fig 4.2). The power of olefin metathesis to prepare PBd-derived materials with diverse architectures and properties has been well demonstrated. Conversely, the numerous problems with the previous REMP strategy for cyclic PBd in our group precluded our efforts to generate the quantity and quality of material necessary to properly elaborate our synthetic methodology and to study bulk properties.⁹

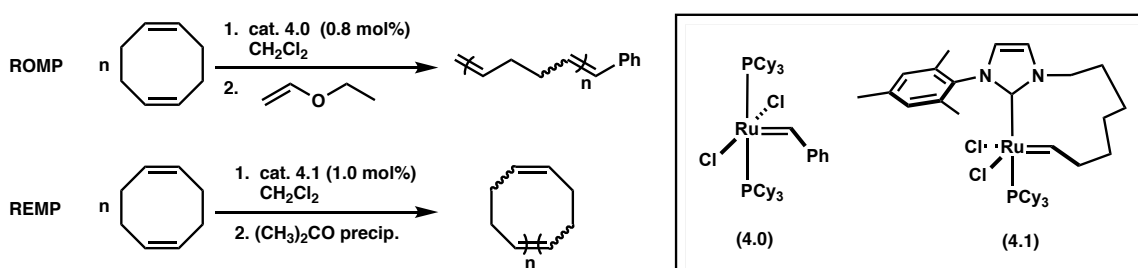


Figure 4.2 | The ROMP¹⁰ (top) and REMP⁸ (bottom) of COD by catalysts **4.0** and **4.1** (top), respectively.

With the success of the supported molecular REMP catalyst **4.2** described in the previous two chapters, we sought to expand our methodology such that multi-gram quantities of cyclic polymers could be reliably produced. A third party expressed interest in acquiring 50 g of cyclic PBd for bulk property analysis and we felt confident in our ability to fulfill their request. This chapter will discuss the design and implementation of large scale REMP methodology for the synthesis of cyclic PBd, complemented by thorough characterization of physical properties, including topological purity.

4.2 – Results and Discussion

Olefin metathesis can produce PBd from a variety of monomers, including cyclobutene, cyclooctadiene, and cyclododecatriene (CDT). That is, any cyclic oligomer of cyclobutene will produce PBd (COD is a dimer, CDT is a trimer, etc.), although they will have drastically different polymerization profiles due to the range of ring strain and steric profiles they encompass. We considered these monomers as we designed the methodology necessary to produce 50 g of cyclic PBd and 50 g of linear PBd, which were both requested by a third party (Fig 4.3, top). Our exploration of the reactivity of REMP catalyst **4.2** described in the previous chapter was again chosen for cyclic PBd, our new target; ROMP catalysts **4.3** and **4.4** were chosen for the linear PBd we also targeted (Fig 4.3, bottom). Catalyst **4.3** was the state-of-the-art ROMP catalyst and catalyst **4.4** was the closest available analog to **4.2**.

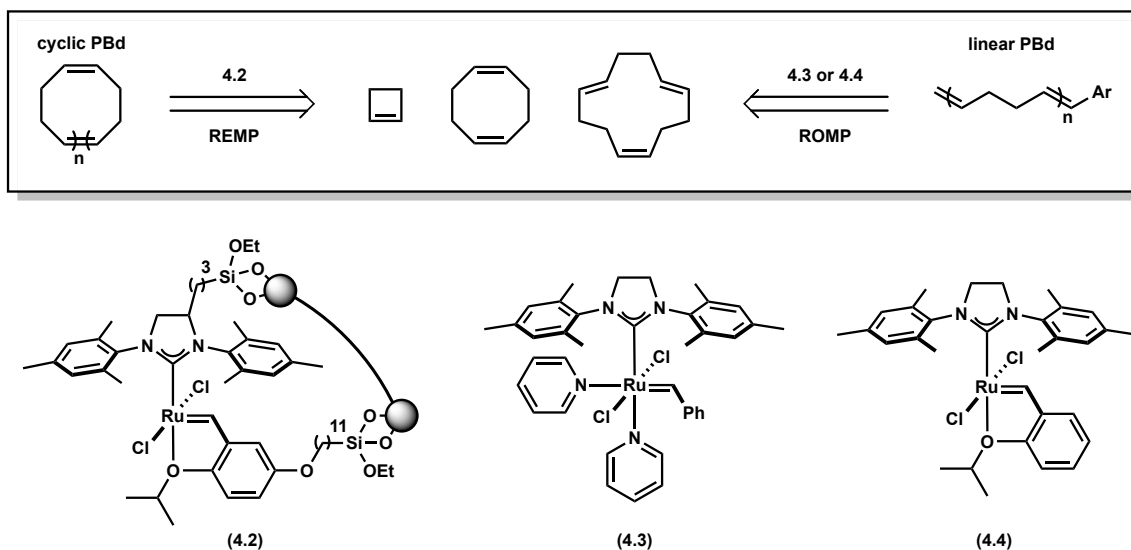


Figure 4.3 | Cycloolefin monomers which produce cyclic (top, left) and linear (top, right) PBd via olefin metathesis catalysts **4.2** – **4.4** (bottom).

Small-Scale REMP and ROMP

The high concentration necessary for COD polymerization leads to a dramatic viscosity increase of the reaction medium as the polymerization proceeds. The filtration process required to isolate cyclic PBd from catalyst **4.2** demanded that we closely monitor the viscosity of the polymerization medium so that filtration would not become untenable. This viscosity increase was indistinguishable between cyclic and linear PBd, so although different catalysts were used, the polymerization profiles of linear PBd ROMP were instructive in the design of cyclic PBd REMP experiments.

Previous efforts to produce cyclic PBd from COD with supported molecular REMP catalyst **4.2** (described in Chapter 3) led us to consider other monomers. We eventually realized the source of our initial COD REMP problems likely arose from trace 4-vinyl-cyclohexene present in our monomer stock. We had not found

evidence of this chain transfer agent present in these experiments, but we did observe signs of radical crosslinking, which 4-vinyl-cyclohexene mediates, particularly when incorporated into the PBd backbone. Although the COD used had been purified by distillation, the extent to which its purity impacted material properties, including cyclic purity, were not originally appreciated. As such, all monomers used in this chapter were extensively purified (see experimental section).

We chose COD over cyclododecatriene and cyclobutene because of the former's poor reactivity and the latter's operational difficulty, since it is a gas at room temperature. Once ultra-pure COD was prepared, small-scale ROMP and REMP optimization experiments were used to establish the reaction parameters and experimental procedures which would be used in large-scale PBd synthesis (Fig 4.4).

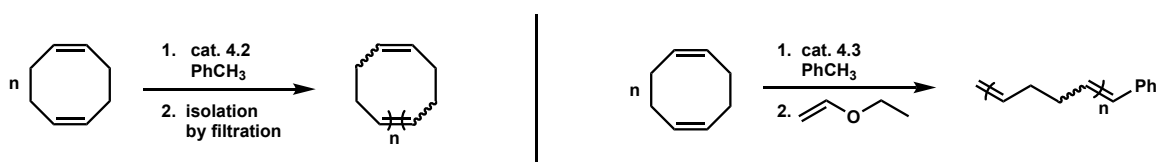


Figure 4.4 | Small-scale REMP (left) and ROMP (right) experiments.

Olefin metathesis catalysts for ROMP are well known to provide excellent MW control and narrow D for polynorbornene and other high ring-strain monomers. Through rigorous experiment design, they can also provide similarly desirable material properties with low and intermediate ring-strain monomers

such as COE, COD and CP.^{13,14} The ratio of $[\text{monomer}]_0:[\text{catalyst}]_0$ determines the degree of polymerization (n), and thus MW, during ROMP, particularly with high ring-strain monomers. Naturally, we explored this method to control the MW of PBd during ROMP and REMP of COD (Figs 4.5 and 4.6).

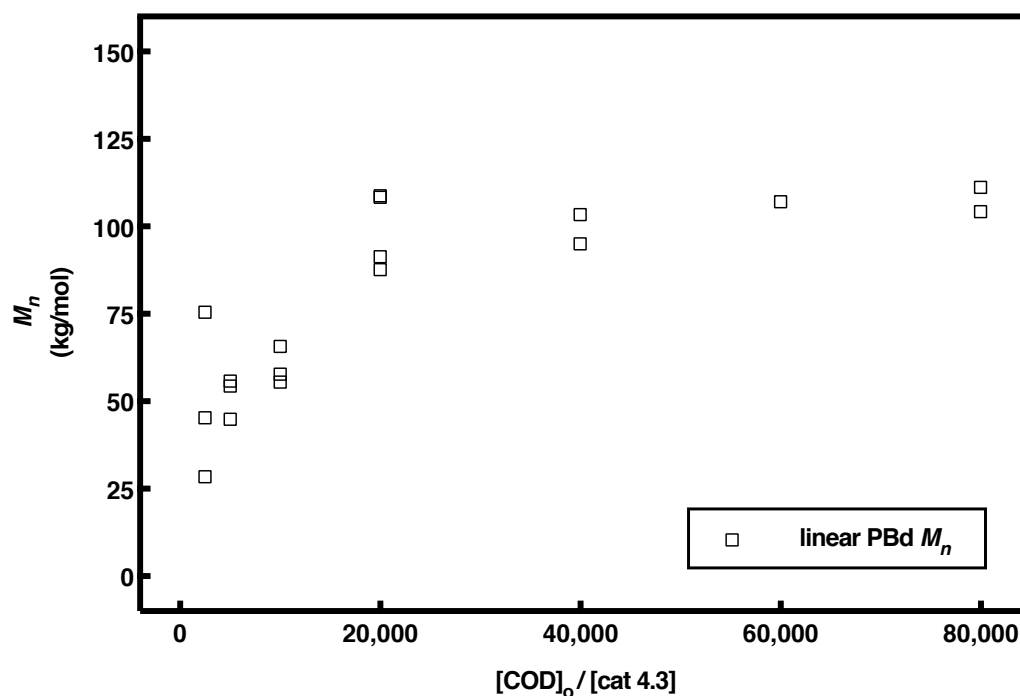


Figure 4.5 | M_n vs. catalyst loading for ROMP of COD to linear PBd.

The relationship M_n vs. $[\text{monomer}]_0:[\text{catalyst}]$ is linear for ROMP of norbornene-based monomers whereby each catalyst produces one chain. The ring-strain of the monomer, and steric bulk along the backbone, prevent depolymerization completely, and thus secondary metathesis events which broaden \mathcal{D} and reduce M_n cannot occur.

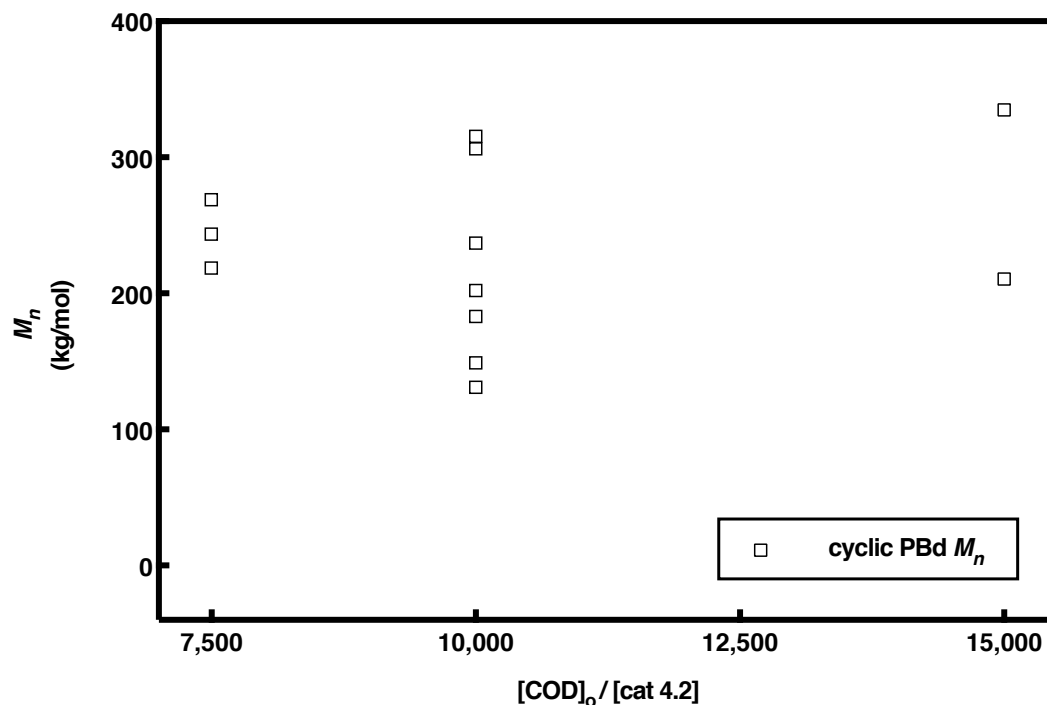


Figure 4.6 | M_n vs. catalyst loading for REMP of COD to cyclic PBd.

A non-linear relationship for ROMP of COD by catalyst **4.3** was observed (Fig 4.5), although the $[\text{monomer}]_0:[\text{catalyst}]_0$ could still be exploited to target a specific M_n , based on purely empirical findings; i.e., M_n was somewhat predictable once an array of variables were explored (non-linear regression $R^2 = 0.7335$, not shown). Conversely, no predictive model was obtained for analogous REMP experiments (Fig 4.6). A linear regression of this data provided the best fit, albeit an extremely poor one, with $R^2 = 0.03$ (not shown). Clearly, reproducibility of COD REMP with catalyst **4.2** proved challenging. The heterogeneous nature of REMP using **4.2** was certainly the fundamental reason for the lack of reproducibility, a theme which will be evident throughout this chapter.

The ROMP of norbornene-based monomers provides quantitative yields with near-perfect reproducibility. We found the ROMP of COD to provide high yields (> 90%), with good reproducibility (Fig 4.7). Conversely, the yield for COD REMP to cyclic PBd with **4.2** was erratic and irreproducible (Fig 4.8), although a generally negative trend between yield and catalyst loading was somewhat evident. Despite sincere efforts, conditions and procedures to enhance reproducibility could not be established. Due to time constraints, we elected to proceed with large-scale REMP experiments without further optimization.

Large-Scale REMP and ROMP

We needed to design a new experimental process to produce 50 g of cyclic PBd because common polymerization procedures were unsuitable: conventional glassware could not accommodate the recycling of catalyst **4.2**, a reactor with a flat surface was required due to the heterogeneity of REMP catalyst **4.2**, and a fritted filtration disc integrated into the reactor would be required to separate cyclic PBd from the catalyst. We incorporated these design principles into the schematic of a custom reactor which was fabricated by Rick Gerhart (Caltech Glassblowing Facilities) (Fig 4.9, left) such that our catalyst recycling process (Fig 4.9, right) could produce the requisite quantity of cyclic PBd (50 g). This scale would constitute a 50-fold increase from our group's previous capabilities up to that point.

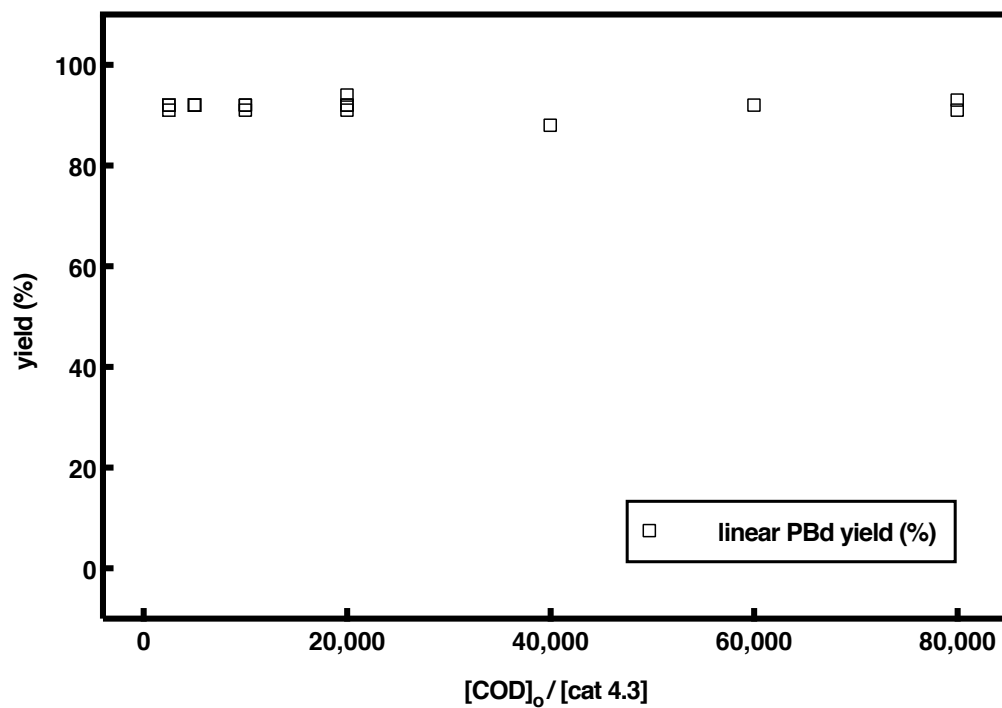


Figure 4.7 | Yield vs. catalyst loading for ROMP of COD to linear PBd.

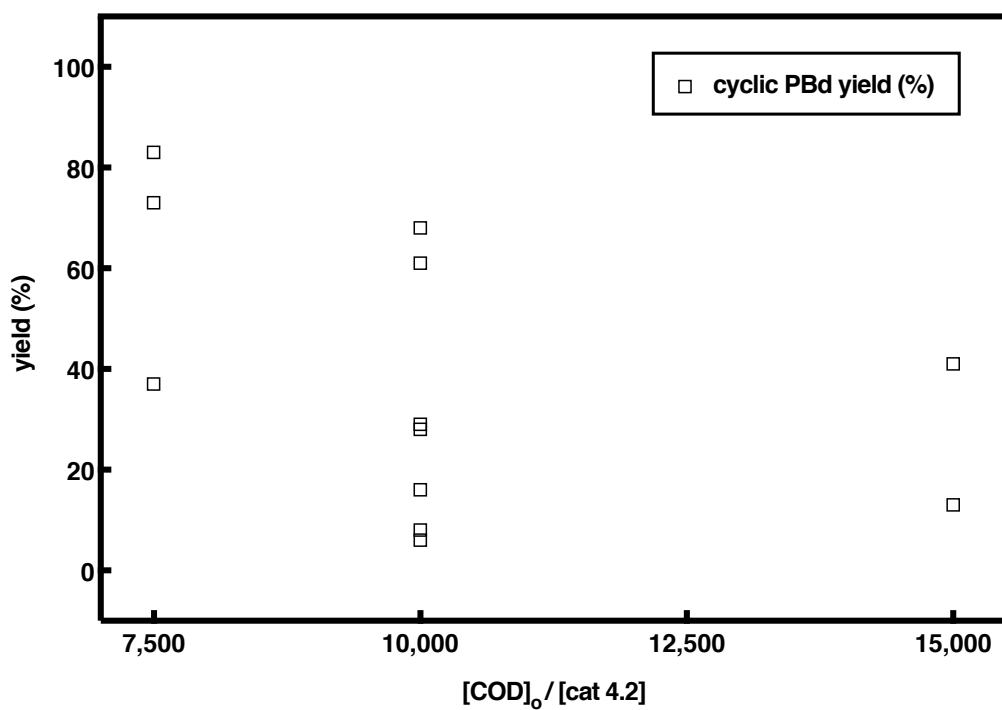


Figure 4.8 | Yield vs. catalyst loading for REMP of COD to cyclic PBd.

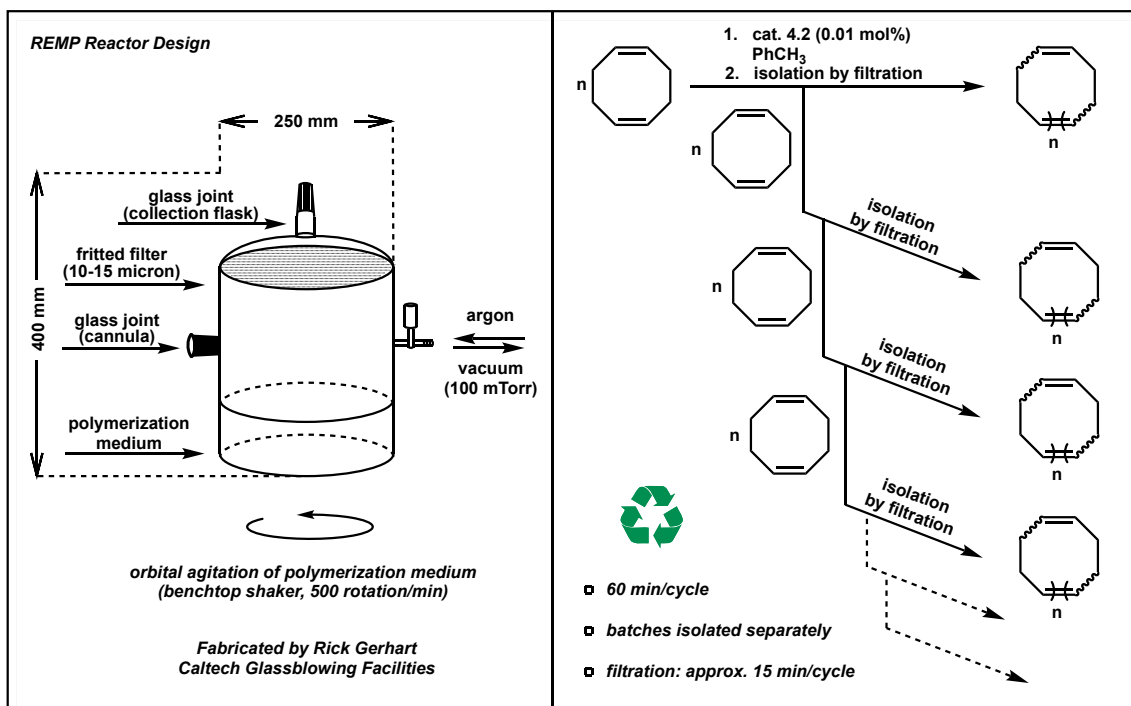


Figure 4.9 | REMP reactor design (left) to accommodate a catalyst recycling process (right).

The first large scale REMP reaction succeeded in producing multi-gram quantities of PBd for each cycle, with 6 total cycles performed. The M_n of each cycle remained reasonably constant throughout the entire recycling process, shown by the range of 210 – 245 kDa for each cycle (Fig 4.10, top). The decrease in yield throughout the process (Fig 4.10, bottom) likely arose from a gradual decline in activity of catalyst **4.2**. Although yields were not excellent for the later cycles, this experiment was certainly a success overall: the 6 cycles cumulatively produced 50.5 g PBd.

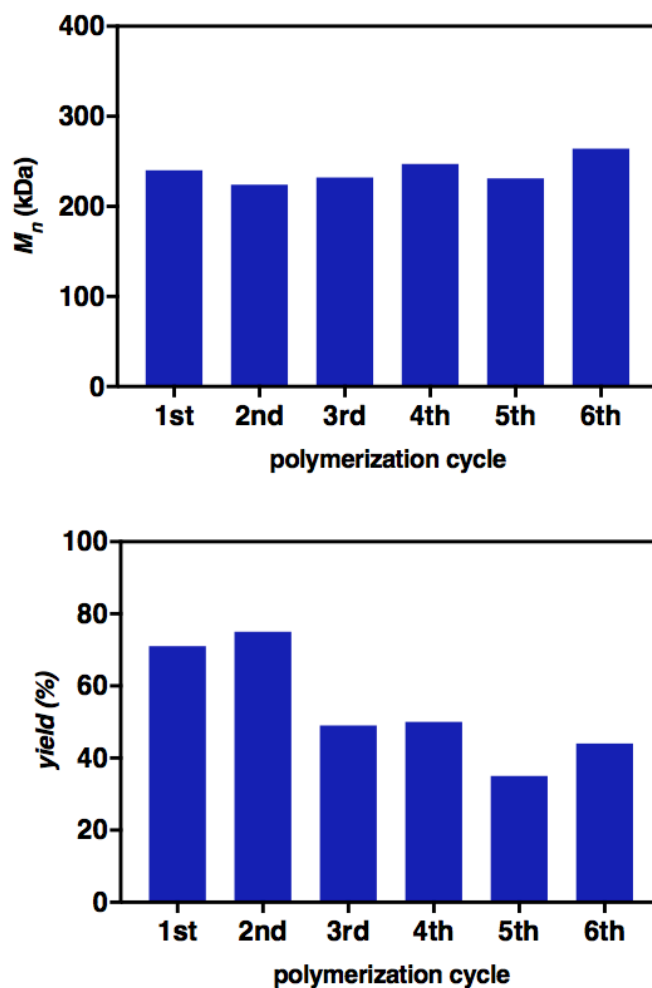


Figure 4.10 | The M_n (top) and yield (bottom) for each of the batches produced in the large-scale REMP recycling experiment.

GPC indicated that each cycle exhibited very similar elution profiles, and each cycle contained substantial low MW material (elution time 15 – 18 min, Fig 4.11), which led to $D > 2$. Although not an explicit requirement from the third party that requested the material, we elected to precipitate the cycles in order to lower the D so that the material would be easier to study. We precipitated our PBd into MeOH 3 total times, which greatly improved D , although approximately 20% of our material was lost in the process (Fig 4.12). We then performed another

recycling experiment, but with only 4 cycles, in order to produce sufficient material. The results from this second large scale recycling experiment corroborated the trends we saw previously: M_n remained mostly unchanged, and yields gradually decreased (Fig 4.13). Additionally, the elution profiles by SEC appeared reasonably consistent for each cycle. After precipitation of these 4 cycles, we obtained the requisite 50 g of cyclic PBd for the third party, as well as sufficient material for IC analysis.

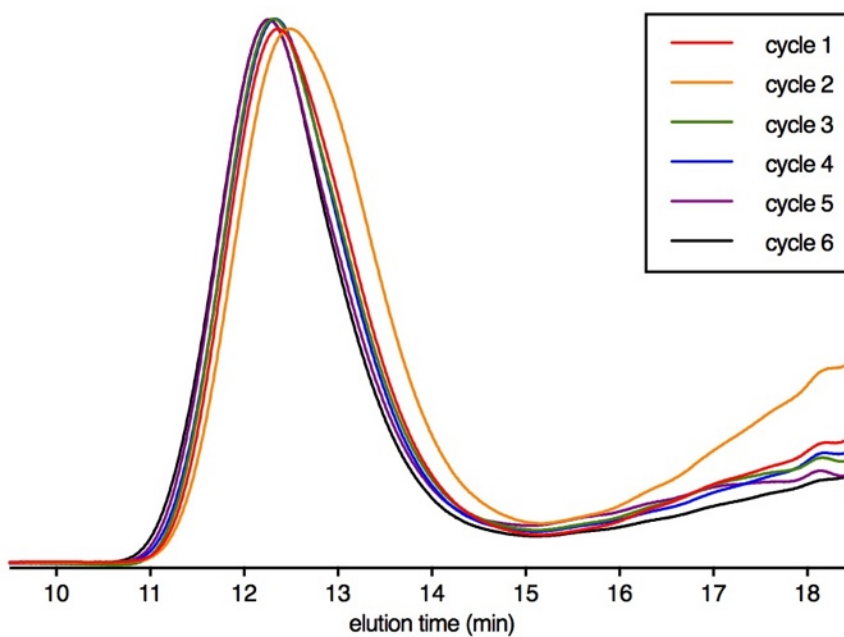


Figure 4.11 | The elution profiles of each PBd cycle.

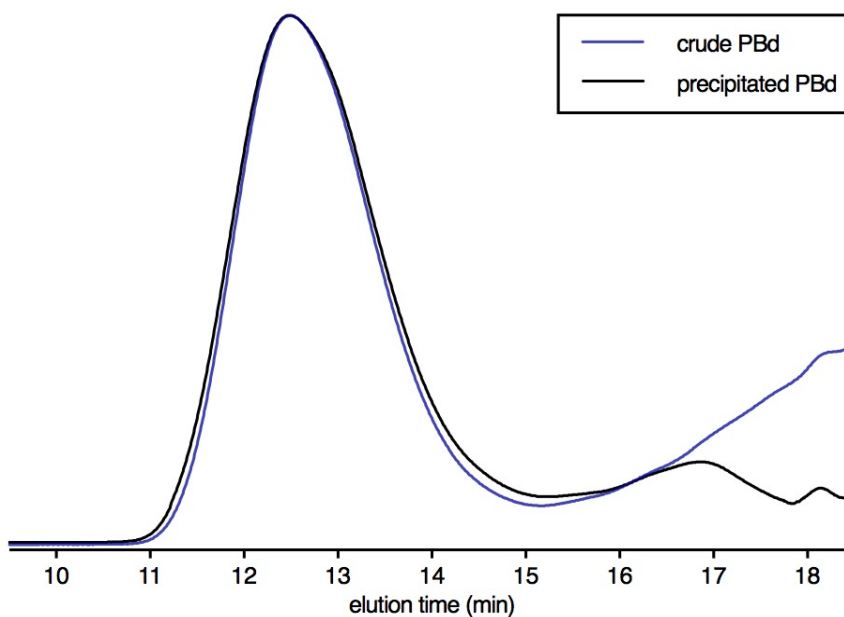


Figure 4.12 | The GPC elution profiles for the crude PBd produced from cycle 2 (blue line), and the same sample after it was precipitated (black line).

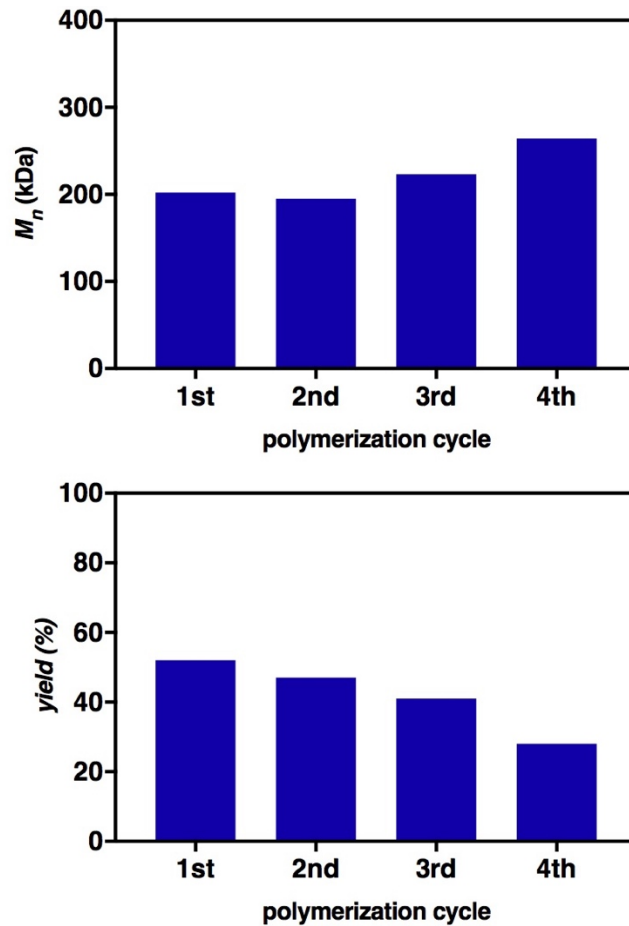


Figure 4.13 | The M_n (top) and yield (bottom) for each of the batches produced in the second large-scale REMP recycling experiment.

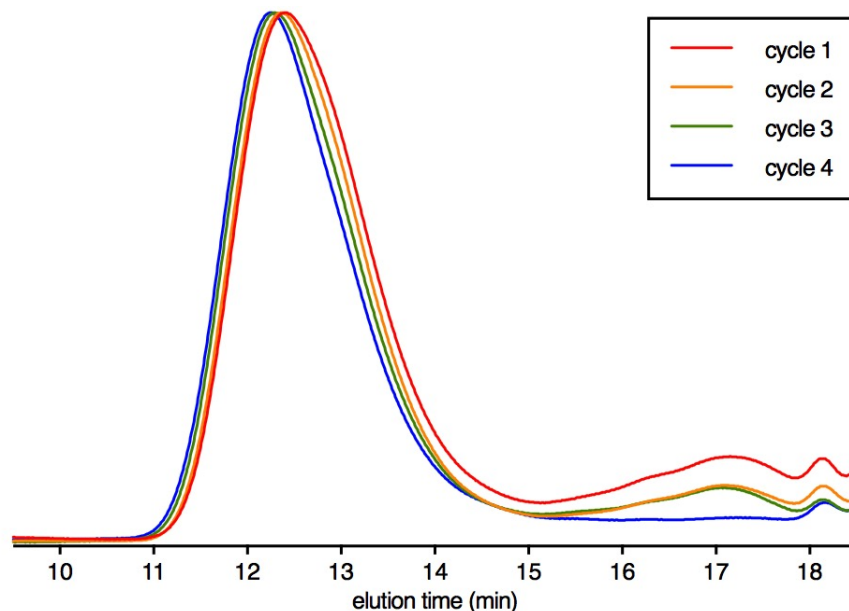


Figure 4.14 | The elution profiles of each PBd cycle in the second recycling experiment.

The IC profiles for cyclic PBd, produced via the large-scale REMP process described above, and linear PBd, produced with catalyst **4.1**, were distinct (Fig 4.15). A bimodal distribution of topologies is clearly seen for ROMP-derived PBd, but a monomodal distribution is observed for REMP-derived PBd. During the ROMP of COD, back-biting inevitably results in cyclic chains within the largely linear population of chains, which explains the bimodal distribution seen for ROMP-derived PBd. That is, our linear PBd also contains a measurable quantity of cyclic chains. This demonstrated both the high purity of our cyclic PBd, and the merit of IC in ascertaining the topological homogeneity of macromolecules.

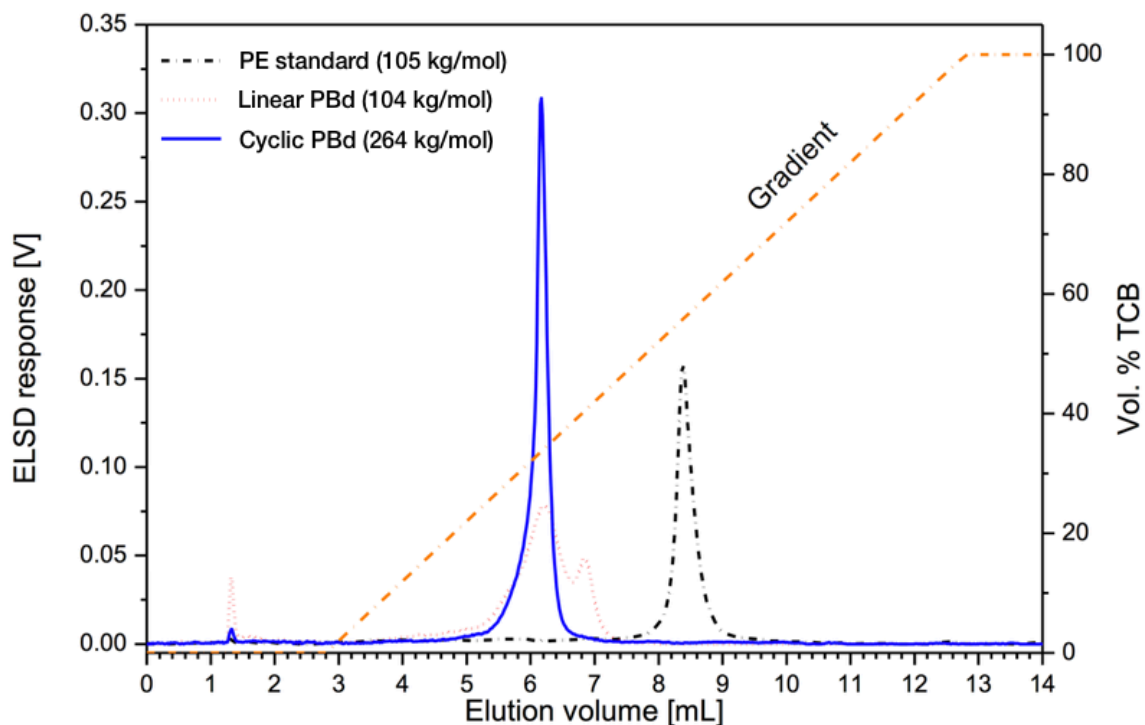


Figure 4.15 | Interaction chromatography elution profiles for cyclic (blue) and linear (dotted red) PBd, as well as a PE standard (dotted black). The solvent gradient of 1-decanol/1,2,4-trichlorobenzene (TCB) is also shown vs elution volume (dotted orange).

At the conclusion of this project, we realized that our cyclic PBd was high-*cis*, as much as 80% by ^{13}C NMR, whereas all PBd we produced via ROMP was 20% *cis*, the thermodynamic ratio. Furthermore, we observed a concentration dependence for the *cis/trans* ratio, which we had not found with ROMP using similar conditions (Fig 4.16). We then began an investigation into the *cis/trans* selectivity afforded during REMP by cat **4.2**, which will be described in detail in Chapter 5 of this dissertation.

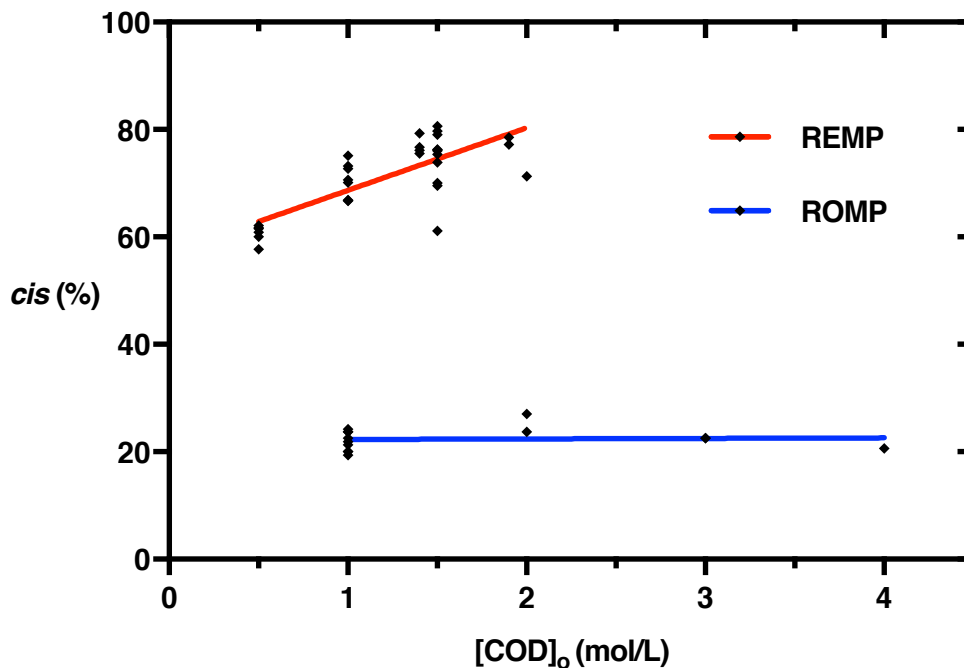


Figure 4.16 | The concentration dependence of the cis content of COD-derived PBd from REMP with catalyst **4.2** and ROMP with catalysts **4.0-4.1**.

4.3 – Conclusions and Future Outlook

The importance of PBd and the potential uses of cyclic PBd were discussed. We developed a strategy to solve a long-term goal of the cyclic polymer project in our group: produce multi-gram quantities of highly pure cyclic polymer. This was accomplished through a series of small-scale optimization experiments and the design and implementation of a novel large-scale REMP catalyst recycling process. We additionally demonstrated the purity of our cyclic PBd using IC.

4.4 – Experimental

GPC

The molar mass and molar mass dispersity of the polyethylene samples were determined on a PL- GPC 220 High Temperature Chromatograph (Polymer Laboratories, Church Stretton, UK) equipped with a differential refractive index (RI) detector. The polyethylene samples (4 mg) were dissolved in 2 mL of TCB for 1 hr together with 0.025 % BHT which acted as a stabiliser to prevent sample decomposition/degradation. TCB with 0.0125 % BHT was used as the mobile phase at a flow rate of 1 mLmin^{-1} . Three $300 \times 7.5 \text{ mm}^2$ PLgel Olexis columns (Polymer Laboratories, Church Stretton, UK) were used together with a $50 \times 7.5 \text{ mm}^2$ PLgel Olexis guard column and 200 μL of each sample was injected. All experiments in HT-SEC were carried out at $150 \text{ }^\circ\text{C}$. The instrument was calibrated using narrowly distributed polystyrene standards (Polymer Laboratories, Church Stretton, UK).

Interaction chromatography (HT-HPLC)

Chromatographic experiments were performed using a solvent gradient interaction chromatograph (SGIC) constructed by Polymer Char (Valencia, Spain). For solvent gradient elution in HPLC, a high- pressure binary gradient pump (Agilent, Waldbronn, Germany) was utilised. The evaporative light scattering detector (ELSD, model PL-ELS 1000, Polymer Laboratories, Church Stretton,

England) was used with the following parameters: gas flow rate of 1.5 SLM, 160 °C nebuliser temperature and an evaporative temperature of 270 °C. A Hypercarb column (Hypercarb®, Thermo Scientific, Dreieich, Germany) with 100 × 4.6 mm internal diameter packed with porous graphite particles which have a particle diameter of 5 µm (making a surface area of 120 m²g⁻¹) and pore size of 250 Å was used for all HT-HPLC experiments. The column was placed in an oven and the temperature maintained at 160 °C. The flow rate of the mobile phase during analysis was 0.5 mLmin⁻¹. To achieve separation, a linear gradient was applied from 100 % 1-decanol to 100 % TCB within 10 min after sample injection. These conditions were held for 20 minutes before re-establishing 1-decanol to 100 %. For all HT- HPLC analyses a concentration of 1 – 1.2 mgmL⁻¹ was used (approximately 4 mg in 4 mL of 1-decanol) with 20 µL of each sample being injected.

4.5 – References

- (1) Brandt, H. D.; Nentwig, W.; Rooney, N.; LaFlair, R. T.; Wolf, U. U.; Duffy, J.; Puskas, J. E.; Kaszas, G.; Drewitt, M.; Glander, S. *Ullmann's Encyclopedia of Industrial Chemistry*, 1, 2nd ed.; Wiley-VCH: Weinheim, Germany, 2000; Vol. 39, pp 30–32.
- (2) Roovers, J. *Macromolecules* **1988**, 21 (5), 1517–1521.
- (3) Lee, H. C.; Lee, H.; Lee, W.; Chang, T.; Roovers, J. *Macromolecules* **2000**, 33 (22), 8119–8121.
- (4) Cho, D.; Park, S.; Kwon, K.; Chang, T.; Roovers, J. *Macromolecules* **2001**, 34 (21), 7570–7572.
- (5) McKenna, G. B.; Hostetter, B. J.; Hadjichristidis, N.; Fetters, L. J.; Plazek, D. J. *Macromolecules* **1989**, 22 (4), 1834–1852.
- (6) Doi, Y.; Matsubara, K.; Ohta, Y.; Nakano, T.; Kawaguchi, D.; Takahashi, Y.; Takano, A.; Matsushita, Y. *Macromolecules* **2015**, 48 (9), 3140–3147.
- (7) Kapnistos, M.; Lang, M.; Vlassopoulos, D.; Pyckhout-Hintzen, W.; Richter, D.; Cho, D.; Chang, T.; Rubinstein, M. *Nat Mater* **2008**, 7 (12), 997–1002.
- (8) Bielawski, C. W.; Benitez, D.; Grubbs, R. H. *J. Am. Chem. Soc.* **2003**, 125 (28), 8424–8425.
- (9) Xia, Y. *California Institute of Technology* **2010**, 1–208.
- (10) Fraser, C.; Hillmyer, M. A.; Gutierrez, E.; Grubbs, R. H. *Macromolecules* **1995**, 28 (21), 7256–7261.
- (11) Trnka, T. M.; Grubbs, R. H. *Acc. Chem. Res.* **2001**.
- (12) Grubbs, R. H. *Tetrahedron* **2004**, 60 (34), 7117–7140.
- (13) Neary, W. J.; Kennemur, J. G. *Macromolecules*.
- (14) Walker, R.; Conrad, R. M.; Grubbs, R. H. *Macromolecules* **2009**, 42 (3), 599–605.